First principles study of perpendicular magnetic anisotropy in thin-film Co_2MnSi

Lukas Stuelke,[1] Parashu Kharel,[2] Paul M. Shand,[1] and Pavel V. Lukashev[1,#]

[1]*Department of Physics, University of Northern Iowa, Cedar Falls, IA 50614, USA*
[2]*Department of Physics, South Dakota State University, Brookings, SD 57007, USA*

E-mail: pavel.lukashev@uni.edu

Abstract

Among different physical parameters taken into account for practical implementations in the field of spin-based electronics (spintronics), magnetocrystalline anisotropy (MCA) and spin polarization play a particularly important role. The former determines the orientation of magnetization direction, while a high degree of the latter is required for producing a spin-polarized current, a cornerstone of spintronics. Due to the miniaturization of the modern electronic devices, one often needs to consider physical effects associated with reduced geometry. In particular, in magnetic thin-film materials, MCA may take a form of perpendicular magnetic anisotropy (PMA), which could be beneficial, e.g. in magnetoresistive random-access memory (MRAM). Yet, combining PMA with half-metallicity may be a challenging task, since the latter is usually destroyed in thin-film geometry (e.g., due to the emergence of surface states), while the former is most pronounced in reduced geometry, because of the contribution to MCA from surface anisotropy. Here, we theoretically explore the nature of PMA in the thin-film full Heusler alloy Co_2MnSi. This material was extensively studied in the past, and it is one of the first compounds for which a half-metallic electronic structure was experimentally confirmed. In addition, it has been reported that this alloy may exhibit perpendicular magnetic anisotropy in thin-film geometry. Here, by analyzing the site-projected magnetocrystalline anisotropy energy (MAE), we confirm that both PMA and surface half-metallicity are very sensitive to the termination surface and mechanical strain. In particular, while MnSi-termination under compressive strain may retain both 100% spin-polarization and out-of-plane magnetization orientation, Co-termination has a detrimental impact on both. These results may serve as a guide for practical applications in the field of spin-based electronics.

I. Introduction

Among various physical phenomena exploited in the emerging field of spintronics, generation of highly spin polarized current at room temperature received particular attention in recent years, largely due to the reported half-metallic (HM) electronic structure of certain Heusler alloys, which retain their magnetic properties well above room temperature. The concept of half-metallicity was suggested some four decades ago in a seminal work by R. A. de Groot et al.[1] Since then, many alloys have been theoretically predicted to exhibit 100% spin-polarization (which is a definition of half-metallicity),[2,3] and some HM compounds have been reported experimentally.[4,5] In fact, given a very fast growing number of reports on potentially half-metallic materials, providing even the most representative references is a formidable task, unless that is the main goal of the paper (i.e. review article).[6,7]

Another important physical parameter, which is often studied for spin-based device applications is magnetocrystalline anisotropy. As it determines the orientation of the magnetization direction, it is of particular importance for magnetic data storage applications.[8,9,10,11,12,13,14,15] Such applications often require magnetic materials to be grown as high quality thin films, in which case MCA may take the form of perpendicular magnetic anisotropy, which could be beneficial, e.g., for current-induced magnetization switching in magnetoresistive random-access memory.[16,17,18]

Combining PMA with half-metallicity in thin-film geometry may provide additional functionalities for spintronic devices, yet this may be a challenging task, since half-metallicity is usually destroyed in thin-film geometry (e.g., due to the emergence of surface states),[19] while the out-of-plane magnetization is most pronounced in reduced geometry, because of the contribution to MCA from surface anisotropy.[13] Nevertheless, a few years ago, William Butler and his co-workers showed from first principles that PMA and half-metallicity may co-exist in certain Heusler alloys, grown on MgO substrate.[20] In particular, they predicted such co-existence for Mn-terminated Co_2MnSi. In addition, in our recent work we showed that these two properties may co-exist in a Co_2CrAl thin film, if it has a CrAl-terminated surface.[21]

The full Heusler compound Co_2MnSi has been extensively studied in the past, both experimentally and theoretically. In particular, it is one of the first Heusler alloys for which half-metallicity in thin-film geometry was observed experimentally.[22,23] Prior to experimental confirmation of half-metallicity in Co_2MnSi, it was predicted theoretically with highly accurate

GW calculations.[24] Moreover, perpendicular magnetic anisotropy has been experimentally observed in Co_2MnSi thin films grown on MgO.[25] The main purpose of the current work is to analyze the nature of PMA in thin-film geometry of Co_2MnSi, by employing site-projected magnetocrystalline anisotropy energy calculations. It will be demonstrated that while MnSi-termination under compressive biaxial strain may retain both 100% spin-polarization and out-of-plane magnetization orientation, Co-termination has a detrimental impact on both.

All calculations in this work are performed using techniques implemented in the Vienna *ab initio* simulation package (VASP). The detailed description of the computational methods is reported elsewhere.[21]

The rest of the paper is organized as follows. Section II discusses equilibrium electronic, magnetic, and crystal structures of Co_2MnSi. In Section III, we discuss the calculated ground state site-projected MAE in thin film Co_2MnSi. Section IV presents our analysis on the effect of biaxial strain on calculated site-projected MAE. Section V contains concluding notes, followed by acknowledgments and references.

II. Equilibrium electronic, magnetic, and crystal structures

The physical properties of Co_2MnSi have been extensively studied in the past. In particular, this material has been reported to crystallize in regular cubic structure (Fig. 1(c)), with an equilibrium lattice constant of 5.630 Å; to exhibit half-metallic electronic structure in bulk geometry, with the minority-spin band gap of around 0.90 eV; and to align ferromagnetically, with 5.00 μ_B/f.u. ($\approx$1.00 μ_B/Co and $\approx$3.00 μ_B/Mn). See, e.g., Ref. [24] for theoretical and Ref. [23] for experimental reports.

Although bulk Co_2MnSi is half-metallic in the ground state, the perfect spin-polarization is unfavorably affected in reduced geometry, because of the emergence of surface states. This is illustrated in Figure 2 (left panel), which shows the cell-projected density of states (DOS) for the 64-atom structure shown in Fig. 1 (a) (the in-plane lattice constant is fixed at the bulk value of 5.630 Å). The numbering of the cells in Fig. 1 (a) and Fig. 2 are consistent with each other. The detrimental effect of reduced geometry on spin-polarization is a well-known effect that has been

reported for other Heusler compounds as well.[26,27,19] In fact, a thin-film half-metallicity is rather uncommon, and it was reported for a few materials only.[28,29,23,30]

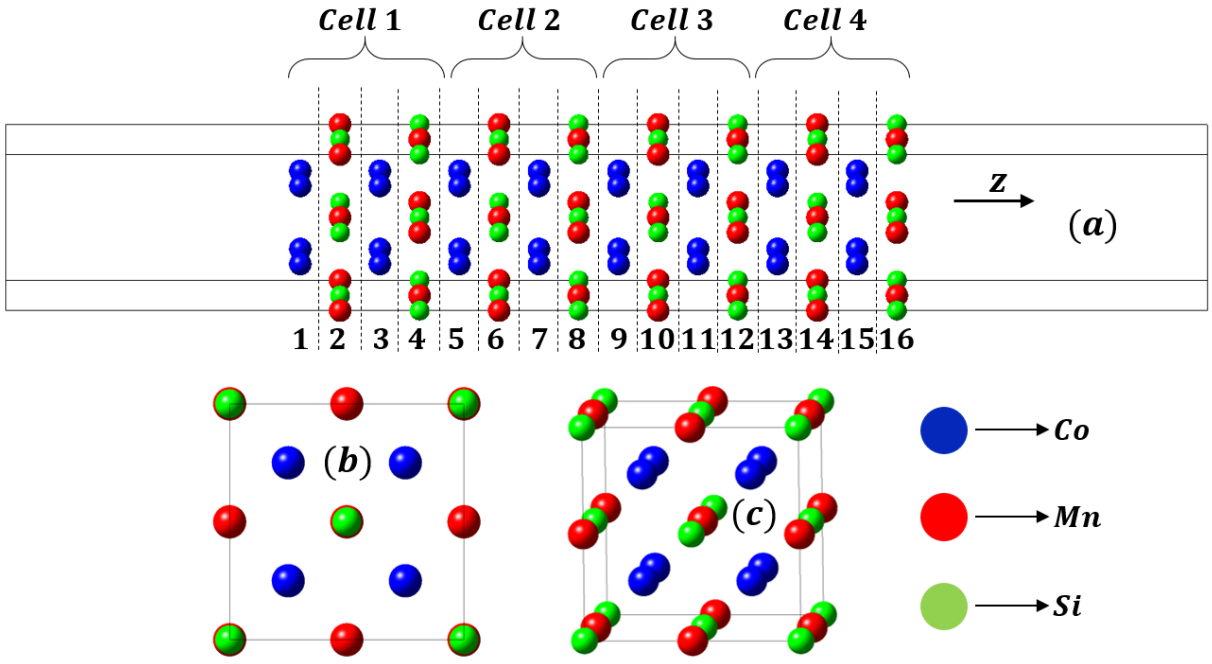

Figure 1: (a) schematic view of the 64-atom super-cell of thin-film Co_2MnSi; (b) top view of the super-cell shown in Fig. 1 (a); (c) schematic view of the bulk Co_2MnSi unit cell. Atoms are colored as indicated in the figure: blue – Co, red – Mn, green – Si. The out-of-plane direction (indicated by *z* vector) is shown in Fig. 1 (a).

As illustrated in Fig. 2, although bulk-like Cells 2 and 3 retain a half-metallic behavior, the half-metallicity is destroyed at Co-terminated Cell 1, due to the emergence of minority-spin surface states around the Fermi energy. The half-metallicity is also destroyed at MnSi-terminated Cell 4, but the minority-spin energy gap is retained, indicating a possibility of induced half-metallic transition, e.g. by mechanical strain on a suitable substrate. The right panel of Fig. 2 shows the enlarged version of Figures 2 (a) and (d), highlighting the profile of the minority-spin surface states.

III. Ground state MAE of thin-film Co_2MnSi

The calculated atom-projected MAE of the thin-film Co_2MnSi (see crystal structure in Fig. 1 (a)) is shown in Figure 3 (a). Here, we fixed the in-plane lattice parameter at the bulk value of 5.630

Å, while the out-of-plane atomic positions are not relaxed, i.e. the system retains a cubic symmetry. The site-projected MAE values reported here and in the rest of this work are two times larger than the actual values of the total energy correction to the second order in spin-orbit coupling (SOC).[31] For details of the computational techniques employed to estimate the site-projected MAE, see, e.g., our recent work at Ref. [21]. The calculated MAE of non-magnetic Si atoms is negligible, and is not included in Fig. 3 (a) and in the rest of this work.

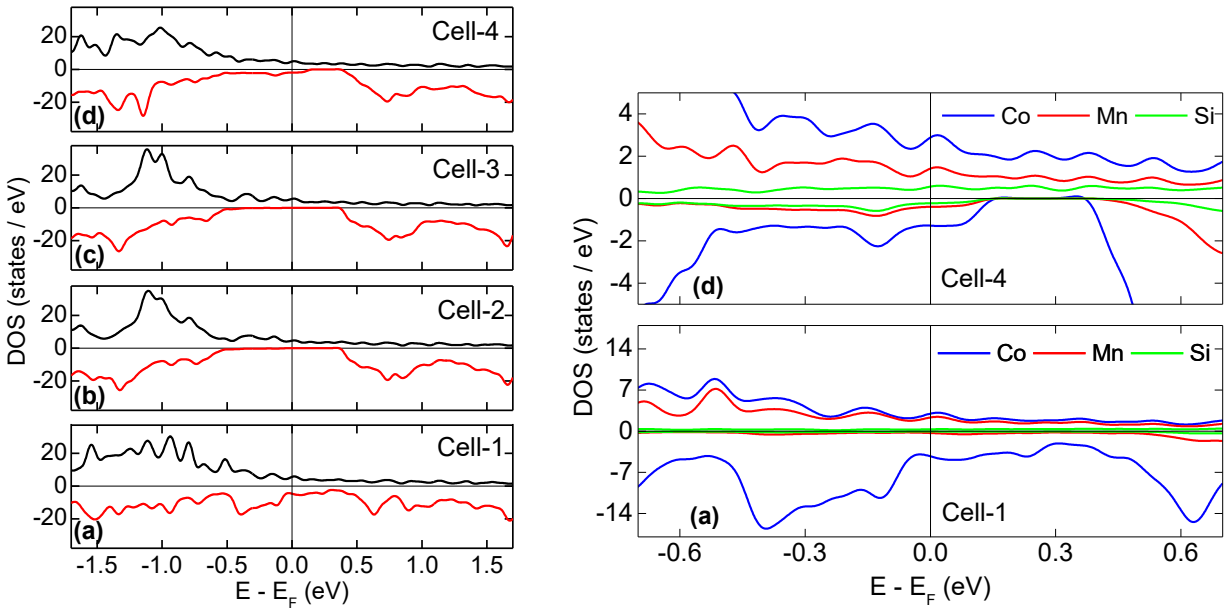

Figure 2: Left panel: Cell-resolved density of states of thin-film Co_2MnSi for the 64-atom cell shown in Fig. 1 (a). Vertical lines indicate the position of the Fermi level. Positive (black line) and negative (red line) DOS correspond to majority- and minority-spin states, correspondingly. The labeling of the cells is consistent with the one shown in Fig. 1 (a). Right panel: Enlarged version of Figures 2 (a) and (d), highlighting the profile of the minority-spin surface states (blue – Co, red – Mn, green – Si).

As shown in Fig. 3 (a), the only sizeable contribution to MAE from Co (blue line and squares) comes from the left surface (see Fig. 1 (a)). In particular, the calculated MAE of Co at the surface layer 1 is around -0.8 meV/Co. Here, the negative number indicates in-plane magnetization orientation, since MAE is estimated as $E(x) - E(z)$ where $E(x)$ and $E(z)$ are calculated energies with magnetization pointing in-plane and out-of-plane, correspondingly.[21]

The calculated MAE of Mn (red line and circles) at the leftmost layer 2 is also negative (-0.6 meV/Mn), which is probably due to the orbital hybridization of Mn atoms of this layer with the surface Co atoms. At the same time, the rightmost surface Mn atoms (layer 16) have positive MAE value of around 0.3 meV/Mn, indicating out-of-plane magnetization orientation.

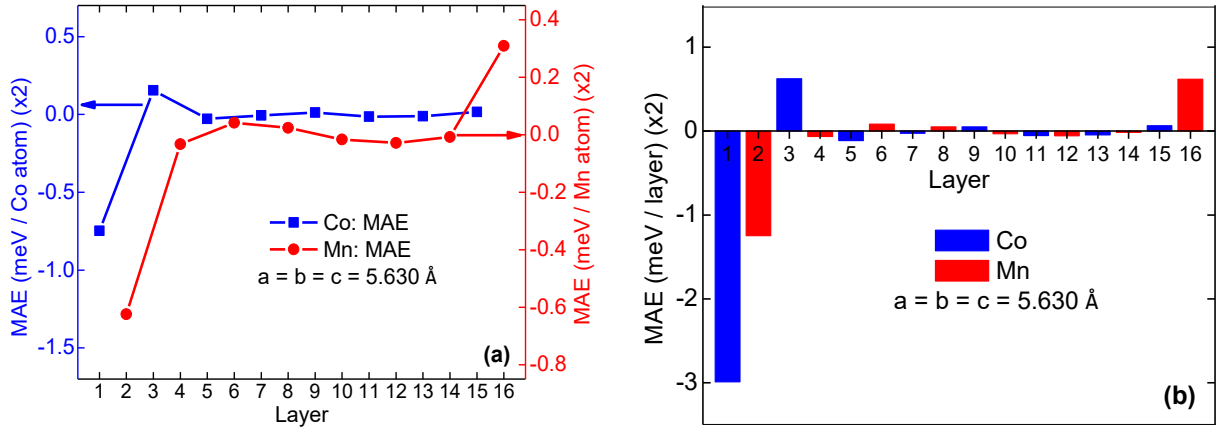

Figure 3: (a) Atom-resolved MAE, calculated at equilibrium in-plane lattice constant. Blue line and squares – Co, red line and circles – Mn. (b) Layer-resolved MAE, calculated at equilibrium in-plane lattice constant. Numbering of the atomic layers is consistent with the one shown in Figure 1 (a). Red columns – Mn layers, blue columns – Co layers.

To better visualize the information presented in Fig. 3 (a), we also plot layer-resolved MAE, which is estimated by calculating total MAE per atomic layers shown in Fig. 1 (a). In particular, the MAE per Mn atom is multiplied by 2, while the MAE per Co is multiplied by 4, where 2 and 4 are the numbers of corresponding atoms per layer shown in Fig. 1 (a). This layer-projected MAE is shown in Fig. 3 (b), which clearly illustrates in-plane magnetization orientation (negative MAE) at the left surface, and out-of-plane magnetization orientation (positive MAE) at the right surface.

IV. Calculated MAE under biaxial strain

For practical device applications, spintronic materials are often need to be grown on a substrate in a thin-film arrangement, e.g., in magnetic tunnel junctions (MTJ).[32] Depending on a

lattice mismatch with the substrate, this may result in a sizable epitaxial strain in the material. It is therefore important to know not only the ground state physical properties of the material, but also how these properties depend on the mechanical strain. This issue is addressed in the current section.

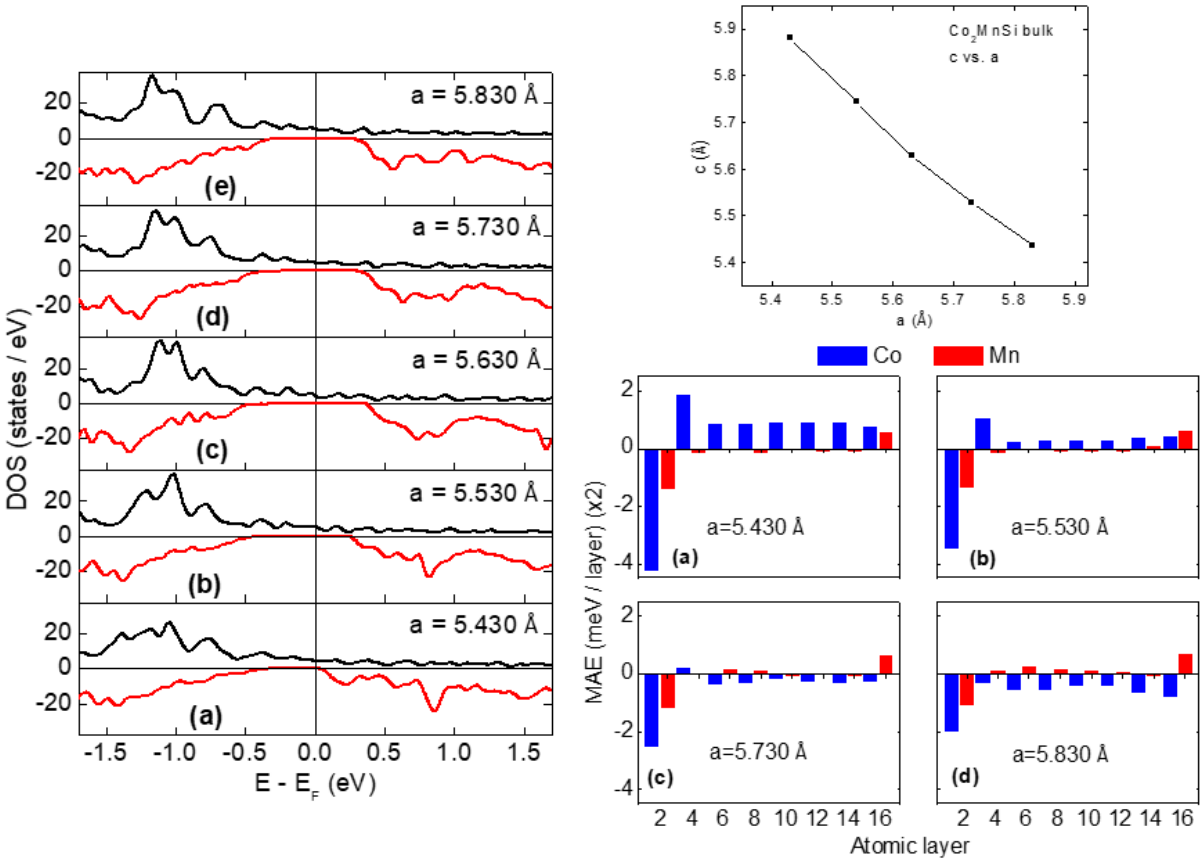

Figure 4: Left panel: calculated density of states of bulk Co_2MnSi under biaxial strain. Right panel: (top) calculated out-of-plane vs. in-plane lattice parameters of bulk Co_2MnSi under biaxial strain; (bottom) layer-resolved MAE, calculated at different in-plane lattice parameters under biaxial strain, with fixed in-plane lattice constants (shown on the figure), and optimized out-of-plane coordinates. Numbering of the atomic layers is consistent with the one shown in Figure 1 (a). Red columns – Mn layers, blue columns – Co layers.

As was mentioned above, although the perfect spin polarization is reduced at the MnSi-terminated surface, the minority-spin energy gap is still retained, which implies a possibility of restoring the half-metallic surface by tuning the lattice parameter, i.e., by external strain. This is

indeed confirmed by our calculations, as illustrated in Fig. 4 (left panel). This figure shows the calculated total DOS of bulk Co_2MnSi under biaxial strain (the calculated out-of-plane vs. in-plane lattice constants (c-vs-a) are shown on Fig. 4 (top, right panel)). As is evident from this figure, the application of compressive strain shifts the Fermi level towards the minority-spin conduction band, and therefore may result in a half-metallic transition in MnSi-terminated thin-film of Co_2MnSi (see Fig. 2 (d)). The question arises, however, of how the application of compressive strain affects the magnetocrystalline anisotropy of this material. Therefore, we next analyze the effect of the biaxial strain on the calculated site-projected MAE. To do so, we fixed the in-plane lattice parameters of the cell shown in Fig. 1 (a) at different values, and for the out-of-plane lattice parameters we selected the optimized bulk values (see Fig. 4 – top, right panel). The results of the layer-resolved MAE calculations are illustrated in Fig. 4 – bottom, right panel.

Application of the biaxial strain naturally breaks the cubic symmetry of the cell. As a result, in addition to the surface MCA, which dominates the calculated MAE in the unstrained cell (Fig. 3), now a sizeable MAE is also exhibited in the "bulk-like" layers, which is a direct consequence of an induced tetragonal distortion. Increase of this distortion, i.e., increase of the biaxial strain, increases the MAE values at the "bulk-like" layers (compare e.g. Fig. 4 (a) (larger strain) with Fig 4 (b) (smaller strain), both shown at the bottom of the right panel). Importantly, these "bulk-like" MAE values are positive for compressive biaxial strain, and negative for tensile biaxial strain. At the same time, the application of a biaxial strain has a minimal effect on the calculated surface MAE values, i.e., the magnetization at the MnSi-terminated surface still points out-of-plane, while the magnetization at the Co-terminated surface is still in-plane. Thus, *under compressive biaxial strain, MnSi-terminated Co_2MnSi may exhibit thin-film half-metallicity along with perpendicular magnetic anisotropy*. It should be noted, however, that for thicker films the contribution of the magnetostatic energy (shape anisotropy) may become decisive, which could result in in-plane magnetization orientation.[21]

V. Conclusions

We performed a thorough computational study of site-projected magnetocrystalline anisotropy energy in thin film Co_2MnSi. It is shown that this material may exhibit a perpendicular magnetic anisotropy, along with 100% spin-polarization, at MnSi-terminated surface, under

compressive biaxial strain. The Co-terminated surface is not half-metallic in the ground state, and no half-metallic transition is induced under external strain. This is due to the complete population by surface states of the minority-spin energy gap at this surface termination. In addition, the Co-terminated surface exhibits in-plane magnetization orientation. Our results therefore indicate that for practical device applications, it may be desirable to grow this material in thin-film geometry with MnSi-termination, under compressive biaxial strain, i.e., at c/a ratios larger than 1. At the same time, tensile strain may not induce a half-metallic transition at the MnSi-terminated surface, and in addition in may induce sizeable negative MAE (in-plane magnetization) in the bulk-like layers of thin film Co_2MnSi.

Acknowledgments

This research is supported by the National Science Foundation (NSF) under Grant Numbers 2003828 and 2003856 via DMR and EPSCoR. This work used the Extreme Science and Engineering Discovery Environment (XSEDE), which is supported by National Science Foundation grant number ACI-1548562. This work used the XSEDE Regular Memory (Bridges) and Storage (Bridges Pylon) at the Pittsburgh Supercomputing Center (PSC) through allocation TG-DMR180059, and the resources of the Center for Functional Nanomaterials, which is a U.S. DOE Office of Science Facility, and the Scientific Data and Computing Center, a component of the Computational Science Initiative, at Brookhaven National Laboratory (BNL) under Contract No. DE-SC0012704. The authors wish to acknowledge the use of the computational resources located at the Pittsburgh Supercomputing Center (PSC),[33] access to which is provided by the Extreme Science and Engineering Discovery Environment (XSEDE), and the computer resources of the Center for Functional Nanomaterials (CFN) at Brookhaven National Laboratory (BNL).

References

1 R. A. de Groot, F. M. Mueller, P. G. van Engen, and K. H. J. Buschow, Phys. Rev. Lett. **50**, 2024 (1983).
2 I. Galanakis, P. H. Dederichs, and N. Papanikolaou, Phys. Rev. B **66**, 174429 (2002).
3 B. Balke, G. H. Fecher, J. Winterlik, and C. Felser, Appl. Phys. Lett. **90**, 152504 (2007).
4 K. Hanssen, P. Mijnarends, L. Rabou, K. Buschow, Phys. Rev. B **42**, 1533 (1990).

[5] W. van Roy, M. Wojcik, E. Jdryka, S. Nadolski, D. Jalabert, B. Brijs, G. Borghs, J. De Boeck, Appl. Phys. Lett. **83**, 4214 (2003).
[6] M. Katsnelson, V. Irkhin, L. Chioncel, A. I. Lichtenstein, and R. A. de Groot, Rev. Mod. Phys. **80**, 315 (2008).
[7] K. Elphick et al., Science and Technology of Advanced Materials, **22:1**, 235 (2021).
[8] B. Dieny and M. Chshiev, Rev. Mod. Phys. **89**, 025008 (2017).
[9] Z. Wen, H. Sukegawa, T. Furubayashi, J. Koo, K. Inomata, S. Mitani, J. P. Hadorn, T. Ohkubo, K. Hono, Adv. Mater. **26**, 6483 (2014).
[10] T. Nozaki, Y. Shiota, M. Shiraishi, T. Shinjo, and Y. Suzuki, Appl. Phys. Lett. **96**, 022506 (2010).
[11] K. Nakamura, R. Shimabukuro, Y. Fujiwara, T. Akiyama, T. Ito, and A. J. Freeman, Phys. Rev. Lett. **102**, 187201 (2009).
[12] O. G. Heinonen and D. V. Dimitrov, J. of Appl. Phys. **108**, 014305 (2010).
[13] J. Zhang, P. V. Lukashev, S. S. Jaswal, and E. Y. Tsymbal, Phys. Rev. B **96**, 014435 (2017).
[14] Y. Wu, X. Xu, J. Miao and Y. Jiang, SPIN, **05**, 1540012 (2015).
[15] Y. Wu, X. Xu, L. Li, Z. Wang, J. Miao, and Y. Jiang, Phys. Status Solidi A **213**, 2780 (2016).
[16] S. Mangin, D. Ravelosona, J. A. Katine, M. J. Carey, B. D. Terris, and E. E. Fullerton, Nat. Mater. **5**, 210 (2006).
[17] O. Boulle, J. Kimling, P. Warnicke, M. Kläui, U. Rüdiger, G. Malinowski, H. J. M. Swagten, B. Koopmans, C. Ulysse, and G. Faini, Phys. Rev. Lett. **101**, 216601 (2008).
[18] S. Yakata, H. Kubota, Y. Suzuki, K. Yakushiji, A. Fukushima, S. Yuasa, and K. Ando, J. Appl. Phys. **105**, 07D131 (2009).
[19] I. Tutic, J. Herran, B. Staten, P. Gray, T. R. Paudel, A. Sokolov, E. Y. Tsymbal, and P. V. Lukashev, J. Phys.: Condens. Matter **29**, 075801 (2017).
[20] K. Munira, J. Romero, and W. Butler, J. Appl. Phys. **115**, 17B731 (2014).
[21] R. Carlile et al., J. Phys.: Condens. Matter **33**, 105801 (2021).
[22] T. Ishikawa, N. Itabashi, T. Taira, K. Matsuda, T. Uemura, and M. Yamamoto, J. Appl. Phys. **105**, 07B110 (2009).
[23] M. Jourdan et al., Nature Communications **5**, 3974 (2014).
[24] M. Meinert, C. Friedrich, G. Reiss, and S. Blügel, Phys. Rev. B **86**, 245115 (2012).
[25] H. Fu, C. You, Y. Li, K. Wang, and N. Tian, J. Phys. D: Appl. Phys. **49**, 195001 (2016).
[26] I. Galanakis, J. Phys. Condens. Matter **14**, 6329 (2002).
[27] I. Galanakis, J. Magn. Magn. Mater. **288**, 411 (2005).
[28] G. A. de Wijs and R. A. de Groot, Phys. Rev. B **64**, 020402(R) (2001).
[29] A. Debernardi, M. Peressi, and A. Baldereschi, Mater. Sci. Eng. C **23**, 743 (2003).
[30] J. Herran, R. Carlile, P. Kharel, and P. Lukashev, J. Phys.: Condens. Matter **31**, 495801 (2019).
[31] V. Antropov, L. Ke, and D. Aberg, Solid State Comm. **194**, 35 (2014).
[32] E. Tsymbal, O. Mryasov, and P. LeClair, J. Phys.: Condens. Matter **15**, R109 (2003).
[33] J. Towns, T. Cockerill, M. Dahan, I. Foster, K. Gaither, A. Grimshaw, V. Hazlewood, S. Lathrop, D. Lifka, G. D. Peterson, R. Roskies, J. R. Scott, N. Wilkins-Diehr, "XSEDE: Accelerating Scientific Discovery", Computing in Science & Engineering, vol.**16**, no. 5, pp. 62-74, Sept.-Oct. 2014.